First-principle study of structural and optical properties of $MgSiSb_2$

S. Benlamari, H. Meradji, and S. Ghemid

Laboratoire LPR, Département de Physique, Faculté des Sciences, Université Badji

Mokhtar, Annaba, Algeria.

Abstract

In this work, we report the results of structural and optical properties of the ternary II-IV-V_2 ($MgSiSb_2$) chalcopyrite semiconductor using the full-potential linearized augmented plane wave (FP-LAPW) scheme in the frame of generalized gradient approximation (GGA). The lattice parameters (*a*, *c*), the internal structure parameter, *u*, describing the position of Mg atom and the (*c/a*) ratio are optimized. The results are in good agreement with theoretical data obtained by using other methods. The linear optical properties namely the real and imaginary parts of dielectric function, refractive index and extinction coefficient are calculated. $MgSiSb_2$ compound is observed to present very weak birefringence.

1. Introduction

The recent investigations on chalcopyrite compounds were mostly motivated by their potential use in non-linear optical applications **[1]**, visible-light emitters **[2]**, and photodetectors in solar cells **[3-4]**. The material considered in this study is $MgSiSb_2$ chalcopyrite compound for which no experimental measurements or data are available in the literature; may be due to the difficulty to manipulate light containing elements and to beryllium toxicity.

As well, from a theoretical point of view, there are a few works related to Mg based II-IV-V_2 chalcopyrites. Recently, Liwei et al. **[5]** have studied the structural, elastic and lattice dynamical properties of $MgSiV_2$ (V=P, As, Sb), mainly using first principles calculations based on density functional theory (DFT). Moreover, Jaffe and Zunger have predicted structural parameters and band gap for $MgSiSb_2$ using self-consistent band structure methods **[6]**.

In the present work, we study the chalcopyrite $MgSiSb_2$ using Full Potential Linearized Augmented Plane Wave (FP-LAPW) **[7]** method, in the framework of the DFT **[8],** within the Generalized Gradient Approximation (GGA) to determine their structural and optical properties.

The paper is organised as follows: in section 2, we briefly describe the computational methods used in this work. The obtained results for the structural and optical properties, are presented and discussed in section 3. The main conclusion of our work is finally given in section 4.

2. Computational Methods

The present calculations were performed using the full-potential linearized augmented plane-wave (FP-LAPW) method within the framework of the DFT incorporated in the WIEN2K computer package **[9]**.The exchange and correlations interactions are treated by the gradient generalized approximation (GGA) of Perdew–Burke–Ernzerhof (PBE) **[10]**.

In order to achieve energy eigenvalues convergence in band energies, the wave functions in the interstitial regions were expanded in plane waves with a cut-off R_{MT} and a **k** vector. K_{max}=8. R_{MT} and K_{max} denote, respectively, the minimum radius of the Muffin-Tin spheres and the magnitude of the largest k vector in the plane wave expansion.

However, Fourier expanded charge density was truncated at G max=12 (a.u). The Brillouin zone (BZ) is sampled by 40 special *k* points generated with 7×7×7 Monkhorst-Pack meshes **[11],** where the self-consistency is considered to be achieved when the total energy difference between successive iterations is less than 10^{-5}Ryd per formula unit. Our atomic calculations are performed for Mg $2s^2 2p^6 3s^2$, Si $3s^2 3p^2$ and Sb $5s^2 5p^3$. The study of thermal effects was carried out within the quasi-harmonic Debye model implemented in the Gibbs program **[12]**.

3. Results and discussion

3.1 Structural properties

$MgSiSb_2$ ternary compound crystallize in the chalcopyrite structure belonging to the space group $I\bar{4}2d$ (No. 221) **[13]**. As shown in figures 1, the atoms occupy Wyckoff positions 4a(0,0,0), 4c(0.5,0.5,0) and 8d(u,0.25,0.125); where "**u**" is an internal parameter denoting the dimensionless anion displacement which is given by the following expression:

$$u = 0.25 + (d_{II-V}^2 - d_{IV-V}^2)/a^2 \quad (1)$$

where $d_{II\text{-}V}$ and $d_{IV\text{-}V}$ are the bond lengths between atoms of the corresponding group.

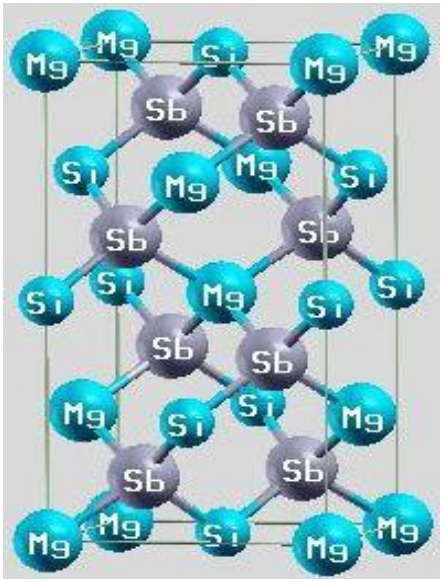

Figure1: Unit cell of MgSiSb2.

The tetrahedron is distorted along the crystal *c*-axis giving rise to deviations of the *c/a* ratio and u from the ideal values of 2.0 and 0.25 respectively.

Thus, the cell energy depends on three geometrical parameters: E = E (a, c, u). The internal parameter, u and the (c/a) rat have been optimized and used as the initial configuration to investigate the structural properties.

The equilibrium geometry and the bulk modulus are then obtained by calculating the total energy at different volumes and by fiting the results to the empirical Murnaghan equation of state **[14]**.

Table 1 presents, for $MgSiSb_2$ chalcopyrite compound, the calculated equilibrium lattice constant a, c/a ratio, distortion parameter u, bulk modulus and bond lengths d_{II-V} and d_{IV-V}, together with some available theoretical data for comparison **[5, 6]**. Both crystals are predicted to be rather close to the ideal twice a zinc-blende cell with c/a ~ 2 and u ~0.25. In general, our results are in reasonable agreement with those predicted by the pseudopotentials with planes waves approach of Ref. **[5]** and with those obtained by using the potential-variational-mixed-basis (PVMB) method **[6]]**. Moreover, our obtained distances fit rather well with the sum of the previously mentioned empirical radii for tetrahedral covalent

bonding. Thus, $d_{Mg-Sb} \approx R_{Mg} + R_{Sb}$ (with 2.89% variation), $d_{Si-Sb} \approx R_{Si} + R_{Sb}$ (with 3% variation).

Table I: Equilibrium structural properties of $BeSiSb_2$ and $MgSiSb_2$: lattice constant (a in Å), c/a ratio, distortion parameter u, bulk modulus B, and first derivative of the bulk modulus with respect to the pressure B' and II-Sb and Si-Sb bond lengths (d_{II-Sb} and d_{Si-Sb}, in Å).

	A	*c/a*	*u*	*B*	*B'*	d_{II-Sb}	d_{Si-Sb}
$MgSiSb_2$							
This work	6.429	1.870	0.280	42.327	4.414	2.845	2.615
Ref. [15]	6.348	1.828	0.287	-	-	2.818	2.541
Ref. [20]	6.221	1.878	0.281	-	-	-	

3.3 Optical properties

In solid state physics, it is of great interest to know the different ways in which light interacts with matter. Thus, among such interactions we can cite light absorption, transmission, reflection and/or diffusion. The response of materials to alternating fields is measured through the complex dielectric function, for which it is natural to separate the real part from the imaginary one. The latter is related to the interaction of photons with electrons **[16]** and expressed by convention in the following way:

$$\varepsilon(\omega) = \varepsilon_1(\omega) + i\varepsilon_2(\omega) \quad (2)$$

To calculate the imaginary part $\varepsilon_2(\omega)$, of the dielectric function, we consider transitions from occupied to unoccupied bands, in the electronic energy band structure, at high symmetry points in the Brillouin zone **[17]**. From the relationship between the real and imaginary parts of the dielectric function, known in physics as the Kramers-Kronig relation **[18-20]**, we can evaluate the real part $\varepsilon_1(\omega)$.

Figure 2, illustrates, the variation of $\varepsilon_1(\omega)$ and $\varepsilon_2(\omega)$ as a function of photon energy ranging from 0 to 13eV for $MgSiSb_2$ system.

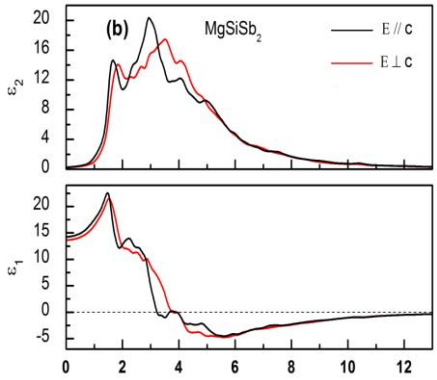

Figure 2: Calculated real $\varepsilon_1(\omega)$ and imaginary $\varepsilon_2(\omega)$ parts of the electronic dielectric function $\varepsilon(\omega)$ of $MgSiSb_2$ for the both polarizations (E∥c) and (E⊥c).

For chalcopyrite structures, there are two independent components of the dielectric function's imaginary part; namely $\varepsilon_{2xy}(\omega)$ and $\varepsilon_{2zz}(\omega)$. The first term is the average of spectra for polarizations along the x and y directions corresponding to the electric field (E) perpendicular to the crystallographic c-axis (E⊥*c*) whereas the second term is related to the z direction corresponding to the electric field (E) parallel to the crystallographic c-axis (E∥*c*).

Figure 2 reveals a difference, between the two components, for energies ranging from 0 to 6 eV, which implies some anisotropic behaviour for the $MgSiSb_2$ system in this range. For energies greater than 6 eV, there is no significant difference, between the two components.

According to figure 2, we expect energy loss to be more important in X-direction than in Z-direction. The main peaks, corresponding to the real part of the electronic dielectric function, present an amplitude which is mainly generated by electronic transitions from the top of the valence band to the bottom of conduction band. Furthermore, figure 2 reveals that the $MgSiSb_2$ system exhibits a peak at an energy of 1.51 eV, with an amplitude of 22.273.

For $MgSiSb_2$, $\varepsilon^{\parallel}(\omega)$ and $\varepsilon^{\perp}(\omega)$ display, each one, a major peak situated at energies of 2.95 eV and 3.55 eV.

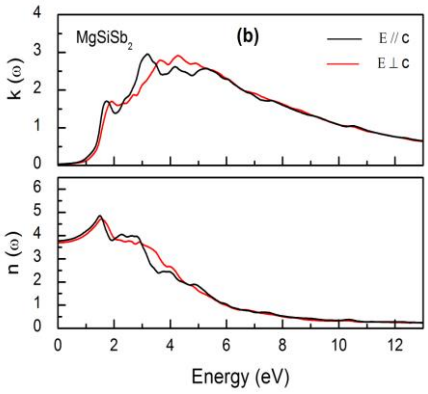

Figure 3: Refractive index n(ω) and Extinction coefficient k(ω), for $MgSiSb_2$ compound.

Figure 3, displays the refractive index n (ω) and the extinction coefficient k (ω) for $MgSiSb_2$, in the basal-plane and along the c-axis direction. The $MgSiSb_2$ system is observed to present an isotropic refractive index for low energies (0 to 2 eV). For energies greater than 2 eV, the refractive index spectrum shows a weak anisotropic behaviour between the extraordinary and the ordinary components. The latter first increase, with energy, reaching maximum values of about 4.71 at 1.56 eV and 4.84 at 1.51 eV are respectively observed, for $n^{\perp}(\omega)$ and $n^{\parallel}(\omega)$. The $MgSiSb_2$ values, of the static refractive indices and the static dielectric functions, are summarized in Table II.

Table II : Static dielectric function and static refractive index

Crystal	$\varepsilon^{\perp}(0)$	$\varepsilon^{//}(0)$	$n^{\perp}(0)$	$n^{//}(0)$
$MgSiSb_2$[	13.64	14.261	3.694	3.776
Ref [6]	14.312	14.715	3.783	3.836

The extinction coefficient k (ω), which is related to the decay or damping of the incident electric field's oscillation amplitude is observed to decrease with increasing incident photon energy.

4. Conclusion

In the present work, equilibrium structural and optic properties have been calculated, for the $MgSiSb_2$ chalcopyrite crystal, by employing the FP-LAPW method, based on the density functional theory (DFT), within the GGA approximation.

The optimized lattice parameters (*a*, *c*) are in reasonable agreement with the few available theoretical data.

To achieve our compounds fundamental characteristics, we have calculated and analyzed their linear optical sensitivities. The real and imaginary parts of the dielectric function, the refractive index, the extinction coefficient and the birefringence have been determined for energies ranging from 0eV to 13eV. The $MgSiSb_2$ dielectric function and refractive index, as well as other important optical properties were found to be nearly isotropic at the low energy.

References

[1] Levine BF (1973) Bond-Charge Calculation of Nonlinear Optical Susceptibilities for Various Crystal Structures, Phys. Rev. B 7:2600–2626.

[2] Shay JL, Schiavone LM, Buehier E, Wernick JH (1973) Spontaneous- and Stimulated-Emission Spectra of $CdSnP_2$, Appl. Phys. Lett. 43:2805.

[3] Wagner S, Shay JL, Migliorato P, Kasper HM (1974) $CuInSe_2$/CdS heterojunction photovoltaic detectors, Appl. Phys. Lett. 25:434.

[4] Kazmerski LL, Juang Y (1977) Vacuum-deposited $CuInTe_2$ thin films: Growth, structural, and electrical properties, J. Vac. Sci. Technol. 14:769–776.

[5] Liwei Shi, Jing Hu, Yun Qin, Yifeng Duan, Ling Wu, Xianqing Yang, Gang Tang (2014) First-principles study of structural, elastic and lattice dynamical properties of chalcopyrite $BeSiV_2$ and $MgSiV_2$ (V = P, As, Sb), J. Alloy. Compd. 611: 210-218.

[6] Jaffe JE, Zunger A (1984) Theory of the band-gap anomaly in ABC_2 chalcopyrite semiconductors, Phys. Rev. B 4:1882-1906.

[7] Koelling DD, Harmon BN (1977) A technique for relativistic spin-polarised calculations, J. Phys. C: Sol. Stat. Phys. 10:3107.

[8] Hohenberg P, Kohn W (1964) Inhomogeneous electron gas, Phys. Rev. B 136: 864-871.

[9] Blaha P, Schwarz K, Madsen GKH, Kvasnicka D, Luitz J (2001) WIEN2k. An Augmented Plane Wave + Local Orbitals Program for Calculating Crystal properties, Vienna University of Technology, Vienna, Austria.

[10] Perdew JP, Burke K, Ernzerlof M (1996) Generalized Gradient Approximation Made Simple, Phy. Rev. lett. 77:3865.

[11] Monkhorst HJ, Pack JD (1976) Special points for Brillouin-zone integrations, Phys. Rev. B 13:5188.

[12] Blanco MA, Francisco E, Luaña V (2004) GIBBS: isothermal-isobaric thermodynamics of solids from energy curves using a quasi-harmonic Debye model Comput, Phys. Commun. 158:57-72.

[13] Hahn T (2005) International Tables for crystallography, vol. A, 5e edition.

[14] Murnaghan FD (1944) Compressibility of media under extreme pressure, Proc Natl Acad Sci USA 30: 244-255.

[15] Kittel C, (1998) Physique de l'état solide Cours et problèmes, 7nd edn, Dunod, Paris.

[16] Sun J, Wang HT, Ming NB, He J, Tian Y (2004) Optical properties of heterodiamond B_2CN using first-principles calculations, Appl. Phys. Lett.84:4544

[17] Saha S, Sinha TP, Mookerjee A (2000) Electronic structure, chemical bonding, and optical properties of paraelectric $BaTiO_3$ Phys. Rev. B 62:8828.

[18] Fox M (2001) Optical Properties of Solids, Oxford University Press, New York, p. 6.

[19] Hufner S, Claessen R, Reinert F, Straub Th, Strocov VN, Steiner P, Ahuja R, Auluck S, Johansson B, Kan MA (1977) Optical properties of PdO and PtO, Phys. Rev. B 50:2128.

[20] Tributsch HZ (1977) Some energetical, kinetical and catalytical considerations verified on MoS_2 layer crystal surfaces, Naturforschung A. 32a: 972-985.